RESEARCH ARTICLE

Preparation and Evaluation of SBA-16, ZSM-5 and MCM-41 Mesoporous Silica Nanoparticles as Drug Delivery System for Carvedilol

Hajir S. Mahdi, Frezah J. I. Muhana, Israa H. Al-Ani, Alaa Al-Sanabrah

Pharmacologic and Diagnostic Research Center(PDRC), Al-Ahliyya Amman University, Amman, Jordan

Received: 31st July, 2022; Revised: 20th August, 2022; Accepted: 03rd September, 2022; Available Online: 25th September, 2022

ABSTRACT

Carvedilol is a non-selective beta/alpha1 blocker that is broadly used in treatment of arrhythmia, congestive heart failure, hypertension, and myocardial infarction. Enhancing carvedilol low solubility and dissolution rate would help in improving the efficiency of the tablet dosage form. In this study, different types of silica nanoparticle (NPs) (SBA-16, MCM-41 and ZSM-5) were synthesized. Coupling of SBA-16 with 3-Aminopropyl-triethoxysilane (APTES) was performed to improve surface characteristics of SBA-16. Different methods to load carvedilol on these carriers were used with high-performance liquid chromatography (HPLC) as a method of analysis for carvedilol. For the characterization of the loaded NPs Fourier -transform infrared spectroscopy (FT-IR), X-ray crystallography (XRD) and Therapeutic goods administration (TGA) were used. MCM-41 loaded with Carvedilol was decided to be formulated as tablet dosage and compared with tablets contain carvedilol without carrier. The results showed that SBA-16, SBA-16 coupled, ZSM-5 and MCM-41 carriers were used successfully to load carvedilol in a good drug load percent of 64.5, 69.3, 82 and 90%, respectively. MCM-41 gave highest loading efficiency of carvedilol using solvent evaporation method and the dissolution of carvedilol from powder was superior to the pure carvedilol where it gave 100% release of the drug at 15 minutes compared to 30% of pure carvedilol. MCM-41 loaded with carvedilol was successfully formulated as tablet dosage form according to the specifications of USP and the release of carvedilol from the prepared tablet was 99% at 15 min compared to the carvedilol released from tablets prepared using carvedilol powder which gave 38% which indicates the efficiency of the carrier in increasing the solubility and dissolution of carvedilol, a class II BCS drugs.

Keywords: Carvedilol, Coupling, Formulation, Nanoparticles.

International Journal of Drug Delivery Technology (2022); DOI: 10.25258/ijddt.12.3.20

How to cite this article: Mahdi, HS, Muhana, FJI, Al-Ani, IH, Al-Sanabrah, A. Preparation and Evaluation of SBA-16, ZSM-5 and MCM-41 Mesoporous Silica Nanoparticles as Drug Delivery System for Carvedilol. International Journal of Drug Delivery Technology. 2022;12(3):1033-1048.

Source of support: Nil.

Conflict of interest: None

INTRODUCTION

Cardiovascular Disease

Cardiovascular diseases (CVD) are among the leading causes of death worldwide. CVDs cover a wide range of disease such as diseases of the vascular system supplying the brain, heart, and other vital organs and of the cardiac muscle.[1] CVD may be considered as a connection that starts with the existence of cardiovascular risk factors and continued via progressive vascular disease to target organ damage, end-organ failure, and death (Dahlöf, 2010).[2] CVDs are a group of disorders of the heart and blood vessels including: coronary heart disease, cerebrovascular disease, peripheral arterial disease, rheumatic heart disease, congenital heart disease, deep venous thrombosis and pulmonary embolism (Figure 1) (WHO, 2021).[3] Modifiable risk factors for CVD including smoking, obesity, hypertension, abnormal lipids, diabetes mellitus, stress, low consumption of vegetables and fruits, and lack of regular physical activity are the main contributors to cardiovascular morbidity and mortality.[2] According to World Health Organization (WHO), in 2019, 32% of all global deaths (17.9 million people) died from CVDs. 85% of these deaths were due to heart attack and stroke.[3] There are several drugs prescribed for patients with heart disease including Angiotensin II receptor blockers (ARBs), Angiotensin-converting enzyme (ACE) inhibitors, Aldosterone inhibitors, Beta-blockers, Calcium channel blockers, Cholesterol-lowering drugs, Diuretics, Digoxin, Inotropic therapy, Vasodilator and others.[4] Beta-blockers is a class of drugs which are commonly used to treat CVDs and other conditions. Beta-blockers got a Food and Drug Administration (FDA) approval for the treatment of hypertension, hyperthyroidism, glaucoma, myocardial infarction, tachycardia, aortic dissection, coronary artery

**Author for Correspondence: f.muhana@ammanu.edu.jo*

disease, congestive heart failure, cardiac arrhythmias, essential tremor, migraine prophylaxis, portal hypertension and other diseases. Beta blockers are used to treat less common conditions including hypertrophic obstructive cardiomyopathy and long QT syndrome.[5] Beta blockers are classified as beta-1 selective and non-selective beta blockers. Non selective beta blockers bind to beta-1 and beta-2 receptors and induce antagonizing effects. Propranolol, carvedilol, sotalol, and labetalol are examples of non-selective beta blocker. Beta-1 selective blockers are cardio selective which bind only to beta-1 receptors such as atenolol, bisoprolol, metoprolol, and esmolol.[5] Carvedilol 1-(9H-carbazol-4-yloxy)-3-[2-(2-methoxyphenoxy)ethylamino]propan-2-ol, was patented in 1978. In 1995, it was approved for medical use in the United States.[6] It is a non-selective β/α1 blocker that is highly used in treatment of congestive heart failure, myocardial infarction, hypertension and arrhythmia.[7] So, carvedilol is an important hopeful drug for cardiovascular diseases. Carvedilol tablets are a prescription drug which are given with food. Carvedilol is available in the market as 6.25, 12.5 and 25 mg tablets. Its starting dose for Left ventricular dysfunction following myocardial infarction is 6.25 mg twice daily and after 3 to 10 days the dose is increased to 12.5 mg then 25 mg twice. Sometimes lower starting dose may be used while in a case of hypertension the starting dose is 6.25 mg twice daily and is increased to 12.5 mg then 25 mg twice daily over intervals of 7 to 14 days if needed.[8,9] Carvedilol is classified as class II drug according to the Bio-pharmaceutic Classification System (BCS). It has high permeability and poor aqueous solubility. Carvedilol is a white to off-white crystalline powder which has very low solubility in water (0.583 mg/L), intestinal and gastric fluids (El-Say and Hosny, 2018; Raju and Murthy, 2011).[7,10] It has low bioavailability which is around 25–35%.[11] The time required to reach the maximum concentration (Tmax) of carvedilol is 1 to 2 hours. Carvedilol has high first-pass metabolism which lead to low bioavailability. Poor water solubility of the drugs impedes at their bioavailability and henders their pharmaceutical development. Pharmaceutical development of drugs with poor aqueous solubility needs the establishing of an accepted formulation layout among different techniques. Several approaches are inspected extensively to improve the water solubility and low dissolution rate of BCS class II and IV drugs. There are several novel formulation options, especially for class II drugs designed for applications like super critical fluid technology, co-crystallization, cyclodextrin complexation, self-emulsification, solubilization by salt formation, change in pH, melt granulation, co-solvents, liposomal/noisomal formulations, solid dispersion, and nanoparticle formation.[12,13] Mesoporous nanoparticles are group of materials that have unique porosities at the nanoscale and show diverse physicochemical properties. These properties are determined by their size, shape and constituent. A spread of those materials is presented with different properties, structures, and applications. the foremost useful technique for the classification of porous nanostructures materials is the diameters of the porosities. IUPAC classified them into three major kinds supported diameters of their pores: Micro-porous (<2 nm), silica meso-porous (2–50 nm), and macro-porous (>50 nm). Between these porous solids, mesopores are simpler than the others because of their high surface areas, thermal and mechanical stability, and tunable porosities. Mesopores materials are employed in various applications like sensors, adsorption, drug delivery systems (DDSs), catalysts, and separation. They're separated into various types such as: Santa barbara amorphous (SBA), Delft university of technology (TUD), Folding shield mechanism (FSM), Mobil composition of Matter (MCM) and Hollow mesoporous silica (HMS) types.[14] Mesoporous nanoparticles (MSN) as a drug carrier have been utilized to improve the dissolution and bioavailability of insoluble drugs.[15] They have been applied for improvement of drug stability, enhancement of drugs activity, responsive release, and for intracellular drugs delivery.[16] Some health conditions require effective, safe and specific treatments, for example: treatment of tumor by chemotherapy relied on the use of very toxic drugs with adverse effects and limited beneficial effects. To solve this issue, targeted drug delivery carriers were designed in order to deliver the required drug doses to the targeted cells with minimum adverse effect profile and maximum efficacy.[17] SBA-16 nanoparticles have a large pore volume, thick pore walls, and a high stability.[18] Thus, it has been employed in drug delivery. As well as it is applied in adsorption, catalysis, and for immobilization of biomolecules.[19] SBA-16 nanoparticles have been used as a carrier system for poor water-soluble drugs. On the other hand, the current literature has few published researches that report the application of SBA-16 in the kinetics of drug release. Actually, more than 40% of new drugs identified as poorly water-soluble and found to have low adsorption and poor bioavailability. In order to solve this problem, high doses of the drug may be given to patients to achieve sufficient therapeutic effects, which may lead to undesirable effects. However, mesoporous silica nanoparticles can overcome such drawbacks of hydrophobic drugs.[20]

MCM-41

MCM-41 have a hexagonal mesopore structure, alterable size and high loading capacity for biologically active substances. These characteristics allowed loading of enzymes or larger drug molecules rising the free volume of the particles (higher degree of drug loading). Furthermore, MCM-41 particles have high physical, mechanical and chemical stability in addition to variable size and mesopores, with the ability to modify the particle surface.[21]

ZSM-5

ZSM-5 is a well-known zeolite. Zeolite occurs naturally but are also produced industrially on large scale. ZSM-5 is an aluminosilicate zeolite with a framework structure containing 10-membered ring channels. The pore dimensions for the two types of channels are about 51 nm, 55 nm and 53 nm, 56 nm, respectively. ZSM-5 is extensively used in catalytic

applications.[22] The first prepared of zeolite ZSM-5 was achieved in 1972.[23] ZSM-5 Nanoparticles represent various advantages in delivery of drugs including increased solubility, protection of drug molecules from degradation, decreased adverse effects and the ability for targeted drug delivery such as zeolite.[24] Carvedilol is class II BCS with low solubility and dissolution rate. Any mean of enhancing its solubility and dissolution rate would help improving the efficiency of the tablet dosage form. Mesoporous silica NP is a DDS that has been used but not widely to improve powder characteristic. But it is known of low loading capacity of medications. Improving loading capacity and the NP efficiency would serve to improve its action as DDS.

METHODOLOGY

Materials

Carvedilol (Shanghai Huiyang Industry Co., Ltd, China), Tetraethyl Orthosilicate (Sigma Aldrich, China), Pluronic 127 (Sigma Aldrich, USA), Myristyltrimethylammonium Bromide (Sigma Aldrich, India), Hydrochloric Acid (Scharlab, European), Deionized Water (Aau Lab), Calcium Chloride Anhydrous (Timstar, UK), Toluene (Tedia, America), Sodium Hydroxide (Sigma Aldrich, Swden), Methanol (Sigma Aldrich, France), 2-Propanol (Sigma Aldrich, France), Ethanol (Labchem Laboratory Chemicals, USA), 3-Aminopropyl Triethoxysilane (Sigma Aldrich, China), Acetonitrile (Carlou Erba Reagents, France), Acetyl trimethyl ammonium bromide tetrapropyl ammonium Hydroxide (Sigma Aldrich, Switzerland), Isopropanol (Sigma Aldrich, France), Alaminium Sulfate Hydrate (Sigma Aldrich, USA), Nitrogen Gas (Gloor, Switzerland), Phosphoric Acid (Carbon Group, United Kingdom), Dichloromethane (Laboratory Chemicals, China), Polyvinylpyrrolidone, K29-32 (Laboratory Chemicals, China), Microcrystalline Cellulose (Laboratory Chemicals, China), Potassium Bromide (Guangdong Chemical Reagents, Chine) and Magnesium Stearate (Laboratory Chemicals, China).

Methods

Synthesis of SBA-16 Nanocarrier

Synthesis of the SBA-16 method was adapted from Thomas *et al*.,[25] The method depends on hydrolysis and condensation of silica precursor as tetraethoxysaline (TEOS) around the micelle template. The template is generated by supramolecular salt-assemblies of surfactant molecules. A 4.0109 g of templating agent (pluronic) was mixed with 30 mL deionized water, 120 g of 2 M HCL was added to the previous solution and was stirred using magnetic stirrer for 30 minutes at 35°C. After that 9.1 mL of tetra ortho silica (TEOS) was added drop by drop to the previous mixture and stirred for 24 hours at 40 rpm. Then the mixture was aged in a water bath at 80°C for 24 hours. After that the mixture was cooled followed by suction filtration to remove solvent and washed by deionized water to get the product. Finally, the powder was dried in oven for 24 hours at 100°C then the surfactant was removed by calcination at 550°C for 6 hours. The target yield was 3 grams.

Synthesis of MCM-41

A 0.4 g of myristyltrimethylammonium bromide was dissolve in 192 mL of water and 1.4 mL of 2 M NaOH at 800 rpm stirring rate and 80°C. When myristyltrimethylammonium bromide completely dissolved. 2.68 mL tetraethylorthosilicate was added and the mixture was stirred for 2 hours at 80°C and 300 rpm. The produced product was collected by centrifugation and washed using water and dried in oven for 2 hours at 60°C. Finally, calcination for 5 hours at 550°C was performed. This method was adapted from .[26]

Synthesis of ZSM-5

Synthesis of ZSM-5 was performed using 12.5 g of terapropylammonium hydroxide dissolved in 50 mL deionized water in a flask, then 12.0 g of tetraethyl orthosilicate was added to the solution flask, after that the flask was placed in a water bath with shaker for 24 hours at 80°C. A solution of 0.24 g sodium hydroxide, 0.722 g aluminum sulfate hydrate, in 4 g deionized water was prepared and added to the previous mixture. The mixture was lined with Teflon and placed in an autoclave for 24 hours at 170°C for crystallization. The molar composition of the gel 1SiO2 : 100 Al2O3 : 0.25 TPAH : 0.5 Na2O : 50 H2O. Finally, the product was collected by centrifugation and calcinated for 6 hours at 550°C. This method was adapted from Hodali and Marzouqa, (2016).[27]

Coupling of SBA-16 with APTES

Coupling of SBA-16 with APTES was aiming to improve surface characteristics of SBA-16. One gram of SBA-16 was dried over night at 110°C to remove adsorbed water. The sample was dispersed with stirring in 50 mL toluene and then 10 mmol APTES was added to the suspension. The mixture was heated for 12 hours under reflux under nitrogen, the resulting product was filtered, washed with toluene 3 times each with 50 mL and then washed with isopropanol (350 mL). The functionalized silicate material was dried at 60°C for 12 hours under vacuum. The optimized ratios for reaction precursors mentioned above were beneficial for increasing the percentage of functionalization. The functionalized products were coded as silicalite-1-NH2.

Loading of Carvedilol on Nanocarrier and Coupled SBA-16

Different methods of loading were used to load carvedilol on SBA-16 and coupled SBA-16 and they were compared to find which was the best method in term of loading efficacy. In all methods the ratio of drug. carrier was 1:1 w/w except in kneading method four ratios were prepared (1:1, 1:2, 1:3 and 1:4) based on the results obtained, while two methods of loading were used to load carvedilol on MCM-41 and ZSM-5. In the solvent evaporation method. ratio of drug: carrier used was 1:1 and 1:2 w/w while in kneading method the ratio used was 1:1.

Adsorption Method

This method was applied on SBA-16 and the coupled SBA-16. For both carriers, 0.1 g of carvedilol and 0.1 g of the carrier

were put in a beaker, then 50 mL of deionized water were added and the mixture was stirred on magnetic stirrer at 40 rpm for 24 hours. Then the sample was dried in oven at 40ºC for 24 hours to remove all water. Samples were collected, sieved through 0.305 mm mesh and kept in a small container in the desiccator until use.

Solvent Evaporation Method

In solvent evaporation method, mesoporous silica nanoparticles were added to a solution of the drug in an organic solvent. The solvent is then removed by fast evaporation such as rotary evaporator to obtain drug loaded mesoporous silica nanoparticles. This method is similar to adsorption but with exception of type of solvent and its removal method.[28] In this method, 0.1 g drug was dissolved in 10 ml methanol in the first beaker then 0.1 g SBA-16 was added and stirred using magnetic stirrer for 24 hours. Also, 0.1 g drug was dissolved in 10 m methanol then 0.1 g coupled SBA-16 was added and stirred using magnetic stirrer for 24 hours. Also, four more samples were prepared using the same method but with different solvent (ethanol and dichloromethane) in addition to methanol.

Physical Mixing

The physical mixing is the simplest mesoporous silica nanoparticles drug loading method. In physical mixing the drug is blended with the mesoporous material in dry conditions.[28] In this method, 0.1 g of drug and 0.1 g of the carrier were mixed using porcelain mortar and pestle for 1-hours. Another sample was prepared by mixing 0.1 g of drug and 0.1 g of the coupled SBA-16 using mortar and pestle also for 1-hour.

Kneading Method

In kneading method, polymers and the drug are triturated using pestle and mortar with addition of liquid dropwise which lead to formation of slurry and decrease in particle size resulting in improved bioavailability.[29] In this method, 0.1 g of carvedilol and 0.1 g of carrier (SBA-16 and coupled SBA-16) were put in a mortar. A solution composed of methanol-water (made acidic by addition of orthophosphoric acid to pH 2) (1:1) was used as kneading vehicle. Drop by drop solvent was added to the mixture until a paste was formed. The paste then was triturated manually for one hour in one direction. The total amount of vehicle used was 2 mL. The paste was then dried in the same mortar in the oven at 40ºC for 24 hours. After drying, samples were scratched from the mortar, sieved and kept in small container until use.

Method of Analysis of Carvedilol

HPLC was used as a method of analyses for carvedilol in all samples and tests. The method was adapted from USP 11 for analysis of carvedilol.[30]

Preparation of Mobile Phase

For each 1 L of deionized water, a volume of orthophosphoric acid was added until it reachs pH 2. The mobile phase composed of solution A (from pump A) Acetonitrile, and solution B (from pump B) deionized water (pH 2) in a ratio 45:55, respectively.

Chromatographic Condition

Chromatographic conditions of the method of analysis of carvedilol is fromServer (LC-Thermo) with by LC Solution Software/Japan, Detector: UV detector, Wavelength: 240 nm, Mobile Phase: Acetonitrile: deionized water pH 2 (45:55), Flow Rate: 1-mL/min, Injection Volume:5 µL, Total Run Time: 6 minutes, Expected Retention Time: 3-5 minutes, Column:EC 250/4.6 Nuclerdur 100 C18ec SN (N21041111), and Column Temp.: 55ºC

Linearity of the Method

Linearity of the method of analysis was tested using 9 concentrations 20, 30, 40, 50, 60, 70, 80, 90, 100 µg/mL. A stock solution of 0.4 mg/mL of carvedilol in methanol was prepared by dissolving 40 mg carvedilol in 100 mL methanol. Suitable dilutions were made to prepare 10 mL of each target concentration. Samples were read using chromatographic conditions mentioned and linear regression was calculated by calculation of R2 (correlation coefficient).

Selectivity of the Method of Analysis

Selectivity of the method was tested by measuring a mixture of carvedilol with the three types of carriers in a ratio of 1:1. Analysis was performed taking 50 µg/mL as target concentration.

Recovery

Recovery of carvedilol from samples containing SBA-16 and coupled SBA-16 was performed by measuring different concentrations from both types of drug-carrier mixtures

Recovery was calculated by the following equation:[31]

$$\text{Recovery } \% = \frac{measured\ concentration}{theoritical\ target\ concentration} x100 \qquad (1)$$

Characterization of the Loaded Nanoparticle

Nitrogen Adsorption Isotherm

Nitrogen adsorption isotherm was determined at 77k with a (Nova 2200e) instrument. The samples were previously outgassed at 120°C under vacuum. The specific surface area BET surface areas, and pore diameters were evaluated through BET and BJH modeling using a nitrogen adsorption/desorption instrument.

Fourier-Transform Infrared Spectroscopy (FT-IR) Study

Instrument used was NEXUS 670 FT-IR (Thermo Nicolet). Small amount (few mg) of each sample was first mixed with KBR in small mortar, then pressed using manual hydraulic press to a small disc. The disc was put in the specified slit in the instrument. The samples were analyzed in the range of 400–4000 cm^{-1} in a resolution of 10 cm^{-1} Results were recorded and analyzed.

X-ray Diffraction

Instrument used was SHIMADZU XRD-7000 XRD.

Thermogravimetric Analysis (TGA)

Thermogravimetric analysis is a method of thermal analysis that measures the mass of a sample over time as the temperature

changes. It is used to determine a material's thermal stability and its fraction of volatile components by monitoring the weight change that occurs as a sample is heated at a constant rate. TGA was conducted using the NetzschSta409 PC instrument (NETZSCH-Ger). TGA was used to analyze of SBA-16 nanoparticles and coupled SBA 16 nanoparticles to confirm the coupling method.

Percent Yield

Each sample of loaded nanoparticle was weighed and after preparation and dried and percent yield was calculated as follows:[32]

$$\%yield = \frac{Mass\ of\ nanoparticles\ obtained}{Total\ mass\ of\ drug\ and\ polymer}\ x\ 100\% \quad (2)$$

Percent Loading of Carvedilol on Nanoparticle

In this part of experiment, 0.05 g of loaded carvedilol nanoparticle powder was dissolved in 100 mL solution composed of 50 mL Distilled water (pH 2) and 50 mL acetonitrile. Sonicator was used until the powder was totally dissolved. 2.5 mL was taken for measurement of carvedilol by the developed HPLC. The concentration and then the amount of carvedilol in the sample was calculated.

%loading was calculated as follow:[33]

$$\%Drug\ loading = \frac{Weight\ of\ drug\ in\ nanoparticles}{Weigh\ of\ nanoparticles}\ x\ 100\% \quad (3)$$

Drug Release from Nanoparticle

This test was performed using ERWEKA dissolution test apparatus Type II (paddle). The USP II method was followed. The media was prepared using 9 mL of HCl and completed to 1.0 L by distilled water then the pH was adjusted to 1.45 using sodium hydroxide and HCL. Then 900 ml of media was added to each jar in the ERWEKA dissolution tester and left for 1 hour at 37°C, 50 rpm before adding the drug to equilibrate with temperature. After 1-hours, a 0.05 g of pure drug powder was added to three jars, 0.11 g of MCM-41 loaded drug which is equivalent to the required amount of drug was added to another three jars and 0.11 g of ZSM-5 loaded drug was added to another 3 jars. Samples were taken at time intervals 5, 15, 30, 40, 50, 60 and 75 minutes, 5 mL from each jar was taken and replaced with 5mL of fresh media. Then each sample was diluted 1:1 using mobile phase and the concentration of dissolved carvedilol was determined using HPLC method.

Formulation of Carvedilol Nanoparticle as Tablet

MCM-41 loaded with Carvedilol was chosen to be formulated as tablet dosage form containing 6.25 mg Carvedilol/ tab. (named F2) and compared with tablets containing carvedilol without carrier with the same amount per tablet (named F1). The aim is to test the efficiency of the carrier to increase the dissolution rate in vitro of a tablet dosage form.

Preparation of Powder Mixture

The two previous mentioned formula F1 and F2 were put in a simple design to avoid many variables that might affect the results. Table 1 shows the component of both formulas.

Table 1: The components of F1 and F2.

Component/Function	*Amount/Tablet in F1*	*Amount/Tablet in F2*
Carvedilol/API	6.25 (mg)	Powder of loaded carrier equivalent to 6.25 mg.
PVP/disintegrant	7.5 (mg)	7.5 mg
Avicel (PH102)/ diluent, disintegrant	131.75	To complete mass to 150 mg
Aerosil/glidant	3.0 (mg)	3.0 mg
Mg stearate/lubricant	1.5 (mg)	1.5 mg
Total Wt.	150 (mg)	150 mg

The powder blend of each formula was prepared by weighing materials enough to prepare 100 tablets. PVP, microcrystalline cellulose (Avicel), colloidal silicon dioxide (Aerosil), and drug (free carvedilol or loaded carvedilol) were weighed, put in conical flask and mixed for 20–30 minutes in one direction. Then magnesium stearate (lubricant) was added and the mixture was studied for flow properties before compression. After evaluation of powder, each formula was compressed to produce the tablets by using Cadmach compression machine.

Evaluation of Powder Mixture

Flowability (Angle of Repose)

The angle of repose is a relatively simple method for assessing the powder flow properties. It can simply determine by letting a powder to flow through a funnel and freely fall onto a surface.[34] In this study, a 7.2 cm diameter and 1-cm orifice funnel were used. The powder poured in the funnel for 15 seconds, and the distance between the lower orifice (height) and the flat surface was 5.0 cm and a ruler was used to measure the height and diameter of the resulted cone.

The Angle of repose θ was calculated from tan θ according to the equation below:

$$\tan\theta = \frac{\text{Height of the powder cone}}{\text{Radius of the powder cone}} \quad (4)$$

Compressibility

Compressibility is the ability of a powder to reduce its volume under pressure[35] and it shows the relationship of bulk density to applied pressure. There are several factors that influence the compressibility such as elasticity, temperature, form, size and water content. The bulk density of materials is important to prevent arching and ratholing effects in silos and hoppers. It is a characteristic value of a compressibility. The Carr index is often used as an indicator for its flowability.[36]

Bulk and Tapped Density

Bulk density was determined by measuring the volume of 14.5 g of powder mixture poured into a 100 mL graduated cylinder without compression according to USP 32 Method I.

Bulk density was calculated in gram per milliliter by Eq. (5):

$$PO = M/VO \quad (5)$$

Where PO is the bulk density in g/mL, M is the mass of the powder in g and VO is the unsettled apparent volume of the powder in mL (USP (919), 2015).

Tapped density was measured by mechanically tapping the cylinder containing the sample by mising the cylinder and allowing it to drop under its own weight in an approximate rate of 200 drop per minute. Tapped density was calculated in gram per milliliter by equation (6):

$$Pf = M/Vf \quad (6)$$

Where P*f* is the tapped density in g/mL, M is the mass of the powder in grams and V*f* the final upped volume of the powder in milliliter.

Carr's compressibility index and Hausner ratio was calculated according to equations below (USP 37, 2014):

$$\text{Carr's compressibility index} = 100\ (Pf - PO)\ /\ Pf \quad (7)$$

$$\text{Hausner ratio} = Pf\ /PO \quad (8)$$

All tests above were performed on both formulas. Three readings were taken and average ±SD was calculated for each.

Powder Porosity

Measuring the porosity of a powder also helps to assess the void volume of the powder. This is reflected in the compressibility and weight consistency of the resulting tablets.

Powder porosity was calculated by the equation (9):

$$\%€ = (1 - Vp/Vb) \times 100 \quad (9)$$

Where, %€ is percentage porosity, Vp is packed volume of the specific weight of powder, and Vb is bulk volume of the powder.

Evaluation of the Prepared Tablets

Tablet Appearance

This test includes visual inspection of the tablet, confirmation of the shape of the tablet, and exclusion of defective tablets such as capping or chipping.

Uniformity of Weight

Weight variation was performed by individually weighing 20 tablets randomly selected from each formulation using an electrically sensitive balance, and the average weight ± SD was calculated (USP 37, 2014).

Tablet Thickness

The thickness test was performed using a thickness caliper for 10 tablets randomly selected from each formulation. Average thickness ±SD recorded.

Hardness and Friability

The breaking force (hardness) was measured with a hardness tester (Copley TBF-1000). Testing was performed at the beginning, during, and at the end of tablet production to ensure a constant hardness throughout the manufacturing process.

Friability of the tablets was determined using friability tester (Labindia FT1020). Twenty tablets were initially weighed (Wtl) and transferred into the Friabilator. The Friabilator was operated at 100 rpm for 4 minutes. The tablets were weighed again (Wt2). The percentage (%) of friability was then calculated using equation (10):

$$\text{Percentage of friability} = \frac{w1 - w2}{w1} \times 100\% \quad (10)$$

Where W1 is the weight of 10 tablets before placing in Friabilator and W2 is the weight of 10 tablets after taking out of Friabilator (USP 37, 2014).

Disintegration Time

Disintegration time was assessed using the disintegration apparatus USP (Copley DTG 2000). Three tablets were used, and each tablet was put in each vessel and time of disintegration was recorded in minutes.

Assay of Carvedilol

Assay of carvedilol in the prepared tablets was performed according to the USP, where 20 tablets were crushed using mortar and pestle. An amount of powder equivalent to 25 mg carvedilol was dissolved in methanol and filtered. A suitable dilution was done to achieve 50 µg/mL. Sample was the measured by the HPLC method and percent carvedilol content was calculated by dividing measured concentration over the theoretical concentration taken as percent. Experiment was repeated 3 times, average and standard deviation was calculated.

Dissolution Test and Drug Release of Tablet

The same method as described in section 3.3.10. In this part, three tablets of carvedilol without carrier (F1) and three tablets of carvedilol-MCM-41-loaded using evaporation method (F2) was added to each to a jar. Samples were taken at time intervals 0, 5, 10, 15, 20, and 30 minutes, 5 mL sample from one jar of each sample type was taken and replaced with 5ml of fresh media. Then each sample was diluted 1:1 using mobile phase and the concentration of dissolved carvedilol was determined using HPLC method. Percent carvedilol released versus time was plotted as the dissolution profile.

RESULTS AND DISCUSSION

Synthesis of SBA-16, ZSM-5, MCM-41 Nanoparticles

The percentage yield was 3.00 g, 2.99 and 2.89 g of SBA 16, ZSM-5 and MCM-41 respectively. Powder of all nanoparticles were white, uniform size (after sieving) and the formation of product was confirmed using FTIR and XRD as described in the characterization section below.

HPLC Method of Analysis of Carvedilol

The peak represents carvedilol appeared at retention time equals to 3.4 min with a resolution more than 5. The peak is sharp, symmetrical with no tailing.

Linearity and Calibration Curve of Carvedilol

Carvedilol linearity was obtained in concentration range between 20–100 µg/mL. Although The International Council for Harmonisation of Technical Requirements for Pharmaceuticals for Human Uses (ICH) guideline set six concentrations as a minimum requirement, in this test 9 concentrations gave a high correlation coefficient. (Figure 6A) illustrate the

calibration curve of pure carvedilol which was done by plotting the measured area vs. concentrations. The linearity R2 was equals to 0.99999 which complies with the ICH guideline.

Selectivity

Selectivity of the method was determined by analysis of mixtures of known concentration of carvedilol with the four prepared carriers using the same chromatographic conditions. No additional peaks appeared using different dilution with no change of the concentration of the known sample.

Recovery

Recovery is proportion of the amount of analyte, present in or added to the analytical portion of the test material, which is extracted and presented for measurement (ICH). A good method would be able to recover the amount of API in from the formula using the same conditions with high accuracy. Recovery of carvedilol from samples contain MCM-41 loaded with carvedilol (prepared by solvent evaporation method), carvedilol- SBA-16 coupling loaded (prepared by kneading method) and ZSM-5 loaded (prepared by solvent evaporation method). Results are listed in Table 2. Recovery of carvedilol in Carvedilol MCM-41 = 97 ± 1.2, Carvedilol SBA 16 = 98 ± 1.0, Carvedilol ZSM-5 = 101.5 ± 1.5.

Characterization of the Loaded Nanoparticle

The carriers and loaded samples were characterized by the result of the following tests.

Fourier-Transform Infrared Spectroscopy

FT-IR spectra were measured over the range 4000 to 400 cm^{-1} using KBr discs. The IR spectra for the samples are shown in (Figures 1ABC) below with the corresponding bands in the Tables (1-4). To explicate the interaction between the carvedilol and MCM- 41 nanoparticle. FT-IR was recorded for the carvedilol, MCM- 41 nanoparticle, and loaded MCM-41. The corresponding bands of drug, MCM-41 nanoparticle and loaded MCM-41 and assignment are listed in (Supplementary Tables 1 and 2 and Figures 1A i, ii, iii) which show distinctive characteristic bands of carvedilol which is consistent with the literature reported data,[37] MCM-41 nanoparticles[38] and loaded MCM-41. Loading of carvedilol into MCM-41 nanoparticle x was supported by the FT-IR- spectrometry. (Table 2) illustrate the presence of carvedilol in the loaded samples. The spectrum of the carvedilol sample Figure 2 i showed absorption bands at 3344.4 cm^{-1} , 3058.2 cm^{-1} and three peaks at 2922.7, 2994 and 2842.5 cm^{-1} characteristics of the N-H, C-H (sp2) and C-H (sp3) stretching, respectively. The presence of an absorption band around 1285.7–1348.2 cm^{-1} confirmed the C-N stretching absorption band, and the stretching absorption band at 1504–1608.1 cm^{-1} duo to C=C bond. Alterations of those representative peaks of carvedilol in the spectrum of the loaded carrier vibration is seen in Figure 1A-iii and Table 2. The (O-H) of nano carrier superimposed with (N-H) peaks of carvedilol in the spectrum, the C=C, C-N, C-H (sp2) and C-H (sp3) peaks to the higher energy, and the absence of peak at 2994 cm^{-1} suggested intermolecular interactions between the carvedilol and the MCM-41 nanoparticle. These spectra supported the postulation of hydrogen bond formation between the hydrogen bond acceptor carvedilol and the proton donor of MCM-41 nanoparticles.

The interaction between the carvedilol and SBA-16 coupled nanoparticle. FT-IR was recorded for the SBA-16 nanoparticle, SBA-16 coupled nanoparticle, carvedilol and loaded SBA-16 coupled. The corresponding bands of SBA-16 nanoparticle, SBA-16 coupled nanoparticle and loaded coupled nanoparticles are listed in (Table 3 and Figures 2A i, ii, iii, iv). Characteristic bands of SBA-16 nanoparticle peaks are similar to peaks reported by Frezah *et al.*,[39] and , SBA-16 coupled nanoparticle are consistent with the literatures reported data.[40] As observed in (Figure 1B ii), in comparison with SBA-16 the FTIR spectrum of coupled SBA-16 shows 2 new peaks at 1560 cm^{-1} and 2920 cm^{-1} , which related to the stretching vibration of C-H and bending of N–H, respectively. The same observation was seen by Ganji *et al.*, (2020).[40] Loading of carvedilol into SBA-16 coupled nanoparticle was supported by the FTIR-spectrometry. illustrate the presence of carvedilol in the loaded samples. The spectrum of the carvedilol sample (Figure 1B-ii) showed absorption bands at 3344 cm^{-1} , 3058 cm^{-1} and three peaks at 2922, 2994 and 2842 cm^{-1} characteristics of the N-H, C-H (sp2) and C-H (sp3) stretching, respectively. The presence of an absorption band around 1285–1348 cm^{-1} confirmed the C-N stretching absorption band, and the stretching absorption band at 1504–1608 cm^{-1} duo to C=C bond. Alterations of those representative peaks of carvedilol in the spectrum of the loaded carrier vibration is seen in (Figure 1B and Supplementary Table 3). The (O-H) of nano carrier superimposed with (N-H) peaks of carvedilol in the spectrum, the C-H (sp3) peaks to the higher energy, presence of SBA-16 coupled nanoparticle peaks at 462, 800 and 1090 cm^{-1} and the absence of peak at 2994 and 3058 cm^{-1} suggested intermolecular interactions between the carvedilol and the SBA-16 coupled nanoparticle. These spectra supported the postulation of hydrogen bond formation between the hydrogen bond acceptor carvedilol and the proton donor of SBA-16 coupled nanoparticle.

FT-IR was recorded for the carvedilol, ZSM-5 nanoparticle, loaded ZSM-5 to explicate the interaction between the carvedilol and ZSM-5 nanoparticle. The corresponding bands of carvedilol, ZSM-5 nanoparticle and loaded ZSM-5 nanoparticle are listed in (Table 4 and Figure 1A i, ii, iii) which show distinctive characteristic bands of carvedilol which is consistent with the literature reported data,[37] ZSM-5 nanoparticles[41,42] and loaded ZSM-5.Carvedilol loaded into MCM-41 nanoparticle was supported by the FT-IR-spectrometry. Table 4 illustrate the presence of carvedilol in the loaded samples. The spectrum of the carvedilol sample Figure 2C-ii showed absorption bands at 3344 cm^{-1} , 3058 cm^{-1} and three peaks at 2922, 2994 and 2842 cm^{-1} characteristics of the N-H, C-H (sp2) and C-H (sp3) stretching, respectively. The presence of an absorption band around 1285–1348 cm^{-1} confirmed the C-N stretching absorption band, and the stretching absorption band at 1504-1608 cm^{-1} duo to C=C

bond. Alterations of those representative peaks of carvedilol in the spectrum of the loaded carrier vibration is seen in (Figure 1C-iii) and Table 4. The (O-H) of nano carrier superimposed with (N-H) peaks of carvedilol in the spectrum the C=C, C-N, and C-H (sp3) peaks to shift higher energy and the absence of C-H (sp2) and C-H (sp3) peaks at 3058 and 2994 cm^{-1} , respectively suggested intermolecular interactions between the carvedilol and the ZSM-5 nanoparticle. These spectra supported the postulation of H-bond formation between the H-bond acceptor carvedilol and the proton donor of ZSM-5 nanoparticles. They could be attributed to a physisorption interactions that exists between the carvedilol and the ZSM-5 in addition to the surface adsorption, which was observed in other systems such as zeolite Y,[43] and montmorillonite.[44]

XRD of Carvedilol, MCM-41, SBA-16, ZSM-5 and Loaded Nanoparticle

XRD of Carvedilol, MCM-41 and Loaded Nanoparticle

The crystalline nature of the carvedilol was confirmed by the XRD pattern (Figures 2E-G with peaks appearing at 6.38, 12.26, 14.90, 19.23, 20.74, 25.96, 26.82 and 38 20 values). The pattern is similar with that reported by Pardhi *et al.*[45] The XRD spectrum of MCM-41. Figure 2E shows a pattern with a strong peak at 2θ of about 2.7 degrees and low intensity peaks at 20 of 4-6 degrees. The pattern is similar with that reported by Cai *et al.*[46] In Figure 2G the chart shows an increase in the intensity of the peak at 2θ of about 2.7 degrees which might referred to the presence of carvedilol crystals in and among silica particles.[47]

XRD of SBA-16 Coupled Nanoparticle

The XRD spectrum of SBA-16 (Figure 2A-D) shows a pattern with a strong peak at 20 of about 0.85 degrees for SBA-16 (Figure 2A) and low intensity peaks at 20 of 18–29 degrees for couped (Figure 2B). The pattern is similar with that reported by Geszke-moritz and Moritz48 at XRD loading pattern of drug and at the same time disappear the two main peaks at 20 of 40°: disappear Figure 2D. This is an indication of carvedilol crystallization in the pores of the nanocarriers. However, the remarkable decrease in crystalline distinctive peaks of loaded carvedilol indicated the less ordered crystallinity than pure drug.

XRD of Carvedilol, ZSM-5 and ZSM-5 Loaded Nanoparticle

The crystalline nature of the carvedilol was confirmed by the XRD pattern with peaks appearing at 20 equal 6.38, 12.26, 14.90, 19.23, 20.74, 25.96, and 26.82 and 38 values. The pattern is similar with that reported by Pardhi *et al.* (2010)[45] for carvedilol. The XRD spectrum of ZSM-5 (Figure 2H) shows a pattern with a strong peak at 20 of about 7–9 and 23–25 degrees, which are specific peaks of ZSM-5 carrier. The pattern is similar with that reported by Cheng *et al.*[49] The XRD spectrum of carvedilol-ZSM-5 loaded (Figure 2M) shows a pattern with a strong peak at 20 of about 7–9 and 23–25 degrees, which are specific peaks of ZSM-5 carrier and another lower intensity peaks at 14.9, 19.23, 20.74, and 25.96 which are specific for carvedilol and at the same time the four main peaks at 20 of 6.38, 12.26, 26.82, and 38 disappear. This is an indication of carvedilol crystallization in the pores of the nanocarriers.

Thermogravimetric Analysis (TGA)

Thermogravimetric analysis is a type of analysis depends on mass, temperature and time. TGA used to separate organic compounds from inorganic, the organic compound will burn while inorganic materials such as silica will not change. The TGA are shown in Figures 3AB of SBA-16 nanoparticles and coupled SBA 16 nanoparticles, respectively. In SBA-16 (Figure 4A) the first region of mass loss (about 1.0%) occurs in temperature range between 20 and 150°C, which could

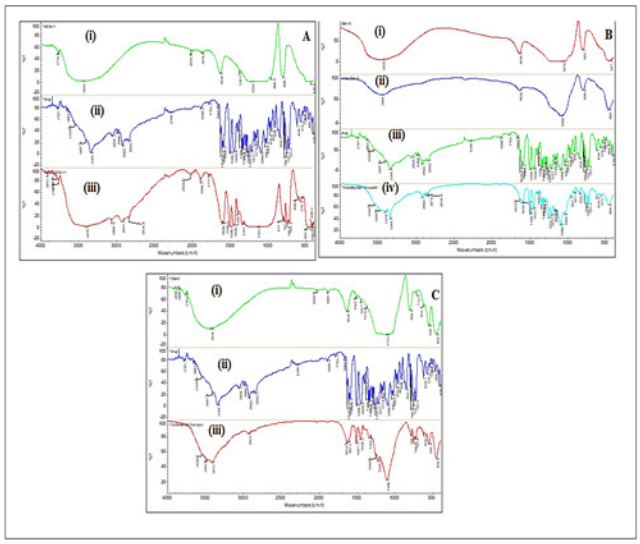

Figure 1: A) Infrared of i) MCM-41 ii) drug iii) loaded drug, B) Infrared of i) SBA-16 ii) drug iii) coupled SBA) vi) loaded drug C) Infrared of i) ZSM-5 ii) drug iii) loaded drug

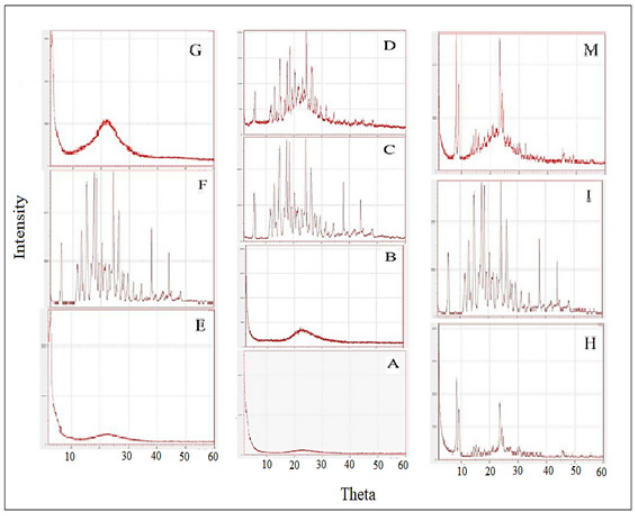

Figure 2: XRD of E) MCM-41 nanoparticle F) carvedilol G) drug loaded MCM-41,A) SBA-16 nanoparticle B) Coupling SBA-16 C) carvedilol D) drug loaded SBA-16, H) ZSM-5 nanoparticle I) carvedilol M) drug loaded ZSM-5

be attributed to the desorption of physically adsorbed water molecules from the silica surface and water bulk molecules occupying within the pores. The second region is attributed to the thermal dehydration of surface silonol groups at 150–1000ºC.[50] Coupled SBA-16 (Figure 3B) in the range of 200–800°C was subjected to 10% weight loss, which noticeably confirmed the successful anchoring of APTES over SBA-16.[51]

PDI, and Zeta Potential and Scanning Electron Microscopy Characterizations of the Synthesized Nanoparticles

The PDI, and zeta potential and scanning electron microscopy characterizations of the synthesized nanoparticles. The size, PDI, and zeta potential of the new nanoformulations were also measured. The results demonstrated that MCM-41, SBA-16 and ZSM-5 formulations were synthesized in nanoscale dimensions with the size of 76.60 nm ± 4.350, 68.06 nm ± 0.000, and 132.8 nm ± 0.8956, respectively. Moreover, the PDI values of the nanoparticles were found to be in of MCM-41, SBA-16 and ZSM-5 of 0.040, 0.039 and 0.215. (Figure 4A-C). The particle size and PDI are critical factors to determine the efficacy of nanoparticles as drug carriers.[52] nanoparticles with PDI values as mentioned above are monodisperse morphology and homogenous.[44] In other hands, particles morphology and size were confirmed also by the scanning electron microscopy (SEM) (Figure 4D-F). Estimates of the sizes. The MCM-41 particles presented homogeneous spherical morphology, with an average diameter of 110 nm. While the SEM images of the SBA-16 synthesis led to a mixture of cubic, faceted and spherical particles with diameters around 5.0 µm. of ZSM-5 was obtained through SEM micrographs. All micrographs depict homogeneous distribution of particles, some of the particles have elongated cubic shapes while others have hexagonal prismatic units with particle size distributions in the range of 0.4–0.8 µm. The result of particle size was found to be in good agreement with the result established by SEM study.

N2 Adsorption/ Desorption Isotherm

Nitrogen adsorption/desorption isotherms were used to estimate the average pore diameter (nm) and specific surface area (m^2/g) for MCM-4, ZSM-5 and SBA-16 nanoparticles (Figure 4A-C). The adsorption isotherm was used for the estimation of surface area by applying Brunauer-Emmett-Teller (BET) theory, while the desorption isotherm was used to estimate the average diameter of the pores by applying Barrett-Joyner-Halenda (BJH) theory. The isotherms for MCM-4, ZSM-5 and SBA-16 nanoparticles are shown in (Figure 5A-C), respectively. The isotherm of MCM-41 showed a distinctive increase in the adsorption curve at a relative pressure P/Po from 0.22 to 0.40, while the range for ZSM-5 is from 0.40 to 0.8, finally the range for SBA-16 is from 0.40 to 0.9. This corresponds to capillary condensation within a uniform mesoporous silicate material. The pore size and surface area for MCM-41 (2.647 nm, 712.1 m^2/g),[53] ZSM-5 (1.232 nm, 360.1 m^2/g)[54] and SBA-16 (3.627 nm, 615 m^2/g)[55] all these results are close to what has been reported in the literature.

Percent Yield of the Prepared Nanoparticle

The percent yield of different nanoparticles using different method of loading and different ratios were calculated. Results are shown in Table 2. Percent yield for all samples was good between 85–96%. The highest percent yield was observed in kneading method while the lowest percent yield was seen in physical mixing method due to the large waste during mixing using pestle and mortar. High quantity was lost on the wall of pestle and mortar and other tools. Mixing may be suitable at large-scale preparation but for small quantity the percent waste will be larger than the final product.

Percent Loading of Carvedilol on Nanoparticle

The percent of drug loaded was calculated after analysis of carvedilol loaded on nanoparticle. As observed in Table 3 the best loading method for SBA-16 was kneading 1:1 w/w while for ZSM-5 and MCM-41 carrier, solvent evaporation method using ethanol was the best method depending on the percent of drug loading. The drug was loaded using kneading method in

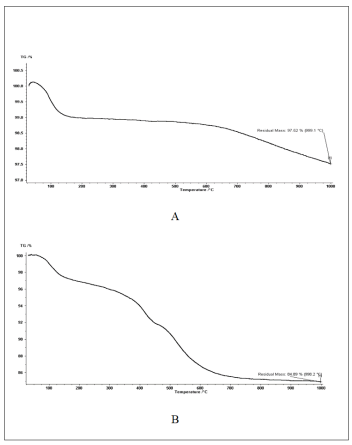

Figure 3: TGA of A. SBA-16 B. coupled SBA-16.

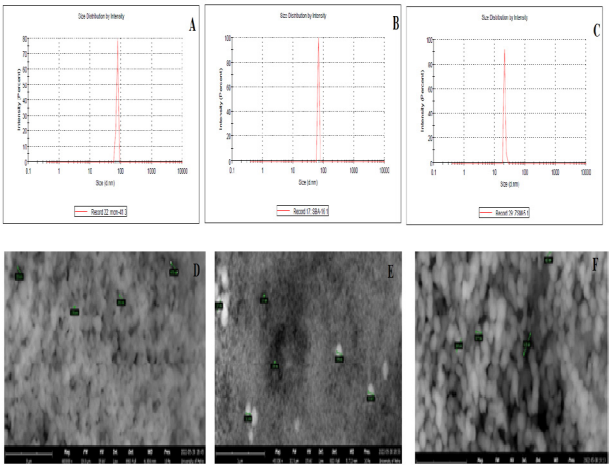

Figure 4: Zeta potential of A) MCM-4, B) SBA-16 and C) ZSM-5 and SEM micrographs of D) MCM-4, E) SBA-16 and F) ZSM-5

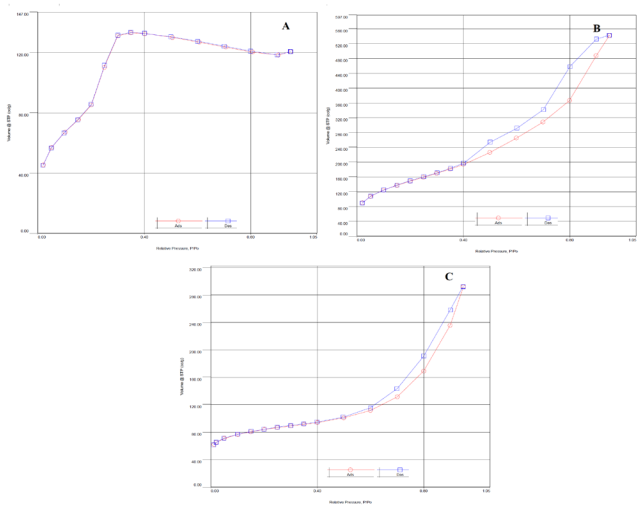

Figure 5: Nitrogen adsorption/desorption isotherm for A) MCM-41, B) SBA-16 and C) ZSM-5.

SBA-16 coupling nanoparticle using different ratios, amount of carrier did not affect the loading efficacy of carvedilol because the carrier will be saturated in carvedilol and no more drug will bond to carrier. Using ethanol in solvent evaporation method was better than other solvent.[28] Assuming that the solvent type is a critical factor in drug loading and the use of less polar solvent (ethanol and hexane) resulting in a higher drug load than more polar solvent (methanol) regardless of solubilization capacity for the drug 28 also maybe the localization of carvedilol in the mesopores was related to the slow introduction of the drug requiring diffusion of carvedilol molecules from an external methanol solution into the nanoparticles. Thus, the solvent evaporation method gives the drug molecules enough time to rearrange and aggregate inside the mesopores.[55]

Drug Release from Powder Nanoparticles

The percent of drug release vs time was plotted in (Figure 6B). After 5 min 67, 38 and 21% of drug was released from carvedilol- MCM-41 loaded, carvedilol ZSM-5 loaded and carvedilol tablet, respectively. In MCM-41 loaded 100% of drug was released after 15 minutes while in ZSM-5 loaded the drug needed 60 minutes to be fully released and it was only 69% released at the same comparison point (15 minutes) with $p > 0.05$. Carvedilol powder was only 33% dissolute at 15 minutes with significantly less than both NPs ($p > 0.05$).

At time 30 minutes, MCM-41 loaded the drug with no more released (100% released in 15 minutes), in ZSM-5 loaded 84% of the drug released while only 40% of drug was soluble from pure carvedilol powder. The rate of drug release was higher in MCM-41 than ZSM-5 nanoparticle significantly ($p > 0.05$).

These results show the efficiency of both types of carriers in increasing *in-vitro* dissolution rate of carvedilol due to large surface area provided by the nanoparticles which enhanced the wettability of the drug and the ability of the carrier to release the drug (especially MCM-41 with the specified

Table 2: Percent yield of carvedilol on different nanoparticles using different method of loading and different ratio.

Carrier	*Method of preparation*	*Ratio*	*Mass of drug+ nanoparticle*	*Mass of product*	*%Yield*
SBA-16	Physical adsorption	(1:1 w/w)	0.2	0.1770	88.5
SBA-16 coupling	Physical adsorption	(1:1 w/w)	0.2	0.1786	89.3
SBA-16	Physical mixing	(1:1 w/w)	0.2	0.1738	86.9
SBA-16 coupling	Physical mixing	(1:1 w/w)	0.2	0.1702	85.1
MCM-41	Kneading	(1:1 w/w)	0.2	0.1818	90.9
ZSM-5	Kneading	(1:1 w/w)	0.2	0.1834	91.7
SBA-16	Kneading	(1:1 w/w)	0.2	0.1802	90.1
SBA-16 coupling	Kneading	(1:1 w/w)	0.2	0.1818	90.9
SBA-16 coupling	Kneading	(1:2 w/w)	0.3	0.2727	90.9
SBA-16 coupling	Kneading	(1:3 w/w)	0.4	0.3604	90.1
SBA-16 coupling	Kneading	(1:4 w/w)	0.5	0.4545	90.9
SBA-16	Solvent evaporation (methanol)	(1:1 w/w)	0.2	0.1904	95.2
SBA-16 coupling	Solvent evaporation (methanol)	(1:1 w/w)	0.2	0.186	93.0
SBA-16	Solvent evaporation (ethanol)	(1:1 w/w)	0.2	0.1914	95.7
SBA-16 coupling	Solvent evaporation (ethanol)	(1:1 w/w)	0.2	0.1922	96.1
SBA-16	Solvent evaporation (dichloromethane)	(1:1 w/w)	0.2	0.1852	92.6
SBA-16 coupling	Solvent evaporation (dichloromethane)	(1:1 w/w)	0.2	0.1904	95.2
MCM-41	Solvent evaporation (ethanol)	(1:1 w/w)	0.2	0.1868	93.4
ZSM-5	Solvent evaporation (ethanol)	(1:1 w/w)	0.2	0.1852	92.6
MCM-41	Solvent evaporation (ethanol)	(1:2 w/w)	0.3	0.2856	95.2

Table 3: Percent of drug loading using different loading method and various nanocarriers.

Nanocarriers	*Loading Method/Ratio*	*% Drug Loading*
SBA-16	Kneading 1:1 w/w	64.50%
SBA-16 coupling	Kneading 1:1 w/w	69.33%
SBA-16 coupling	Kneading 1:2 w/w	56.33%
SBA-16 coupling	Kneading 1:3 w/w	15.0%
SBA-16 coupling	Kneading 1:4 w/w	20.0%
SBA-16	Solvent evaporation (Ethanol)	48.0%
SBA-16 coupling	Solvent evaporation (Ethanol)	62.0%
SBA-16	Solvent evaporation (Methanol)	45.0%
SBA-16 coupling	Solvent evaporation (Methanol)	62.5%
SBA-16	Solvent evaporation (Dichloromethane)	62.5%
SBA-16 coupling	Solvent evaporation (Dichloromethane)	58.5%
SBA-16	Physical mixing	64.0%
SBA-16 coupling	Physical mixing	67.0%
ZSM-5	Kneading 1:1 w/w	74.0%
ZSM-5	Solvent evaporation (Ethanol)	82.0%
MCM-41	Kneading 1:1 w/w	77.0%
MCM-41	Solvent evaporation (Ethanol)	90.0%

method of preparation) without considerable loss or irreversible binding with the API. Weather part of the drug is adsorbed on the surface of the NPs or included inside the pores, both mechanisms acted together to produce smooth release in a very short time.

Formulation of Carvedilol Nanoparticle as Tablets

The promising results of loading capacity and the fast release of carvedilol from MCM-41 NP, it was chosen for the formulation of carvedilol as tablets contain 6.25 mg/tab.

Physical Evaluation of Powder Mixture

Free Carvedilol (F1) and carvedilol-MCM-41-loaded using solvent evaporation method (F2) were prepared to achieve tablet weigh approximately of 150 mg (Figure 6A and B). Concentration of disintegrant was kept 5% and glidant and lubricant approximately 1–1.2% of tablet weight. After mixing, the powder flowability and compressibility were evaluated. Studying flow characteristics of a powder mix is critical for the compression step. Powders of poor flowability characters make difficult compression and, in several times, segregation of powder occurs during compression which might result in non-uniformity of content, poor tablet quality, and variable amount of API from tablet to tablet. The angle of repose was calculated to assess the flow characteristics of the powder blend for each of the prepared formula; these calculated Angle of response properties of Formula F1 and F2 are 34.2° and 30.0° respectively with free flowable. Usually, powder with a value of 0 less than 30° is considered as very freely flowable, between 30–38° free flowable, 38–45 fair, 45–55° cohesive and >55° very cohesive which may not flow.[56] F1 and F2 showed a value

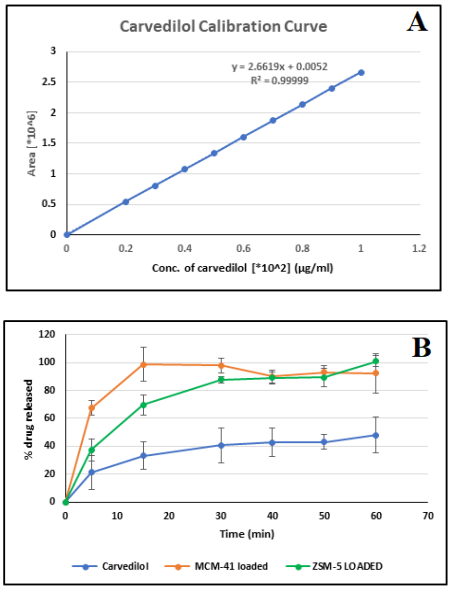

Figure 6: A) Calibration curve of carvedilol B) Percent of drug release for carvedilol, MCM-41 loaded and ZSM-5 loaded.

of which indicates a "free flowable" powder. Bulk density of a powder mix is a result of the density of its constituents. With tapped density they can affect important characteristics like compaction behavior. The more regular particle shape, the more values of tapped density obtained. During compression, the mechanical properties of the powder will affect the quality of tablet obtained with minimum problems. Carr's Index (CI) with Hausner ration (HR) relate the two types of density to flow characteristics and ability of powder to be compressed. The excellent flow properties would have CI < 10 and HR 1- 1.11, while free flow powder would have CI 11-15 and HR 1.12-1.18. A fair powder flow would have CI 16-20 and HR 1.19 - 1.25, passable CI 21-25 and HR 1.26 - 1.34, Poor flow CI=26-31 and above that very cohesive, HR=1.26-1.34 and above that very cohesive powder is present.[57] Results of calculations of density, CI, HR and porosity are represented in Table 4 below. Results comply with the angle of repose measurement where F1 gave "passable" flowability and F2 gave fair powder flow.

The porosity € of powder is the ratio of void volume to the bulk volume of the packaging. Generally, the powder with high porosity would be able to absorb higher amount of water, also to other properties of the powder blend and kind of disintegrant used.[58] During compression the void volume will be reduced but the powder with higher porosity would give tablet of higher porosity and higher capacity of water absorption. Powder mixture of F2 lead to improving the flow properties of the powder in comparison to F1.

Evaluation of Prepared Tablet

Tablet Appearance

The obtained tablets were observed visually. Tablets were good shaped, shinny, smooth with sharp edge and bright white color as seen in Figure 1.

Table 4: Results of flowability and compressibility study (bulk and tapped density, CI, HR and porosity).

Formula	*P°*	*Pf*	*CI*	*HR*	*Flow property*	*Void's volume (mL)*	*Porosity € %*
F1	0.42	0.54	21.42	1.2	Passable	0.12	30
F2	0.5	0.65	16.66	1.2	Fair powder flow	0.15	25

Uniformity of Weight

The average weight of 20 tablets from each formula was measured individually according to the specification of the USP test of weight uniformity test. The results of average weight uniformity test and Percent variation of the F1 and F2 formulas are 152.2 mg, 2.2, 152.4 mg and 2.4 respectively. Tablets weigh less than 180 mg might have less than +10% of weight variation. Tablet's weight 180–325 mg would accept + 7.5% while tablets weigh more than 325 mg would accept ± 5% of its weight variation. No tablet should weigh more or less than double the allowed percent variation. F1 average weight is 150 mg, and it follows the first category while average wight of F2 tablet is 150 mg and it would follow the first category. All tablets were in the USP specifications, and this reflects the efficiency of compression process.

Tablet Hardness, Friability and Disintegration Time

When compressing the tablets, weight and hardness were kept constant. The hardness of the tablet should meet the properties of the immediate release tablet according to the USP, and allow disintegration and dissolution. According to the USP, friability of tablets should not exceed 1% (1% is unaccepted). Therefore, it is necessary to always pay attention to the balance between the control factor (hardness) and the reaction factor (fragility). After several trials in compression of each formulation, the hardness was controlled to give friability below 1%. Results of hardness, friability percent, thickness and Disintegration time of F1 102.6 ± 3.58, 0.68%, 3.88 mm ± 0.03 7:00 minutes while for F2 are 102.2 ± 2.95, 0.70%, 3.92 mm ± 01 and 1:45 minutes respectively. The disintegration time in F2 was much lower than F1 that may be due to the polarity of carrier in F2 which enhances pulling water into pores which lead to faster disintegration.

Assay of the Prepared Carvedilol Tablets

Results of assay of the prepared carvedilol tablets (F1 and F2) according to the USP gave percent of drug 94 ± 1% (F1) and 97 ± 1.2% (F2), both formulas are passed, but the loading of the drug and mixing with carrier and other excipient gave a better distribution which gave a percent nearest to 100% than F1.

Dissolution Test and Drug Release of Tablet

Dissolution of the prepared tablets F1 and F2 were performed according to the USP monograph of carvedilol tablets. Same conditions of powder release were followed. Carvedilol was 99% released from F2 (MCM-41 loaded) in 30 min compared to 45% from F1 which is significantly higher ($p > 0.05$). The same result was obtained from the powder dissolution. The formulation of MCM-41 loaded with carvedilol as immediate-release tablets did not affect negatively the release of the drug from the carrier. Formulation and compression of the loaded carrier kept the superior characteristics of the MCM-41 NP loaded with carvedilol.

CONCLUSION

SBA-16, SBA-16 coupled, ZSM-5 and MCM-41 carriers were used successfully to load carvedilol in a good drug load percent. The percent of drug loading was between 45–64.5%, 15–69.33%, 74–82% and 77–90% for SBA-16, SBA-16 coupled, ZSM-5 and MCM-41, respectively. MCM-41 gave highest loading capacity of carvedilol using solvent evaporation method. The dissolution of powder and tablet dosage form contains MCM-41 loaded with carvedilol was superior for powder and tablet without carrier which indicate the efficiency of the carrier in increasing the solubility and dissolution of BCS class II drugs such as carvedilol.

REFERENCES

1. Gaziano T, Reddy KS, Paccaud, F, Horton, S and Chaturvedi, V. (2006) Cardiovascular Disease. Disease Control Priorities in Developing Countries. 2nd Edition.
2. Dahlöf B. (2010) Cardiovascular Disease Risk Factors: Epidemiology and Risk Assessment. The American Journal of Cardiology, 105, 3A-9A. http://dx.doi.org/10.1016/j.amjcard.2009.10.007
3. WHO. Cardiovascular Disease (CVDs). https://www.who. int/en/news-room/fact-sheets/detail/cardiovascular-diseases- (cvds). 2021.
4. Beckerman J, (2020) Common Heart Disease Drugs. WebMD Medical Reference.
5. Farzam K, Jan A, (2020) Beta Blockers. StatPearls [Internet].
6. Fischer J, Ganellin CR. (2010) Analogue-based Drug Discovery. Chemistry International--Newsmagazine for IUPAC. 2010; 32: 12-15. http://dx.doi.org/10.1515/ci.2010.32.4.12
7. Raju V, Murthy KVR, Development and Validation of New Discriminative Dissolution Method for Carvedilol Tablets. Indian Journal of Pharmaceutical Sciences. 2011; 73: 527. http://dx.doi.org/10.4103/0250-474X.99000 8. FDA. COREG (Carvedilol) Tablets for Oral Use. 2017
8. Takekuma Y, Yagisawa K, Sugawara M, Mutual Inhibition between Carvedilol Enantiomers during Racemate Glucuronidation Mediated by Human Liver and Intestinal Microsomes. Biological and Pharmaceutical Bulletin. 2012;35(2):151-163. Available from: http://dx.doi.org/10.1248/bpb.35.151
9. El-Say K, Hosny K. Optimization of carvedilol solid lipid nanoparticles: An approach to control the release and enhance the oral bioavailability on rabbits. PLOS ONE. 2018;13(8):e0203405. Available from: http://dx.doi.org/10.1371/journal.pone.0203405
10. Morgan T. Clinical Pharmacokinetics and Pharmacodynamics of Carvedilol. Clinical Pharmacokinetics. 1994;26(5):335-346. Available from: http://dx.doi.org/10.2165/00003088-199426050-00002.
11. Chowdary, KPR. Recent Research on Formulation Development of BCS Class II Drugs–A Review. International Research Journal of Pharmaceutical and Applied Sciences. 2013; 3, 173-181. Available from:
12. Kawabata, Wada K, Nakatani M, Yamada S, Onoue S. For-

mulation design for poorly water-soluble drugs based on biopharmaceutics classification system: Basic approaches and practical applications. International Journal of Pharmaceutics. 2011;420(1):1-10. Available from: http://dx.doi.org/10.1016/j.ijpharm.2011.08.032
13. Mirzaei M, Zarch M, Darroudi M, Sayyadi K, Keshavarz S, Sayyadi J et al. Silica Mesoporous Stgructures: Effective Nanocarriers in Drug Delivery and Nanocatalysts. Applied Sciences. 2020;10(21):7533. Available from: https:// doi.org/10.3390/app10217533
14. Izquierdo-Barba I, Sousa E, Doadrio J, Doadrio A, Pariente J, Martínez A et al. Influence of mesoporous structure type on the controlled delivery of drugs: release of ibuprofen from MCM-48, SBA-15 and functionalized SBA-15. Journal of Sol-Gel Science and Technology. 2009;50(3):421-429. Available from: http://dx.doi.org/10.1007/s10971-009-1932-3
15. Han C, Huang H, Dong Y, Sui X, Jian B, Zhu W. A Comparative Study of the Use of Mesoporous Carbon and Mesoporous Silica as Drug Carriers for Oral Delivery of the Water-Insoluble Drug Carvedilol. Molecules. 2019;24(9):1770. Available from: http://dx.doi.org/10.3390/molecules24091770
16. Mirzaei M, Zarch M, Darroudi M, Sayyadi K, Keshavarz S, Sayyadi J et al. Silica Mesoporous Structures: Effective Nanocarriers in Drug Delivery and Nanocatalysts. Applied Sciences. 2020;10(21):7533. Available from:
17. Zhao D, Huo Q, Feng J, Chmelka B, Stucky G. Nonionic Triblock and Star Diblock Copolymer and Oligomeric Surfactant Syntheses of Highly Ordered, Hydrothermally Stable, Mesoporous Silica Structures. Journal of the American Chemical Society. 1998;120(24):6024-6036. Available from: http://dx.doi.org/10.1021/ja974025i
18. Rivera-Muñoz E, Huirache-Acuña R. Sol Gel-Derived SBA-16 Mesoporous Material. International Journal of Molecular Sciences. 2010;11(9):3069-3086. Available from: http://dx.doi.org/10.3390/ ijms11093069
19. Censi R, Di Martino P. Polymorph Impact on the Bioavailability and Stability of Poorly Soluble Drugs. Molecules. 2015;20(10):18759-18776. Available from: http://dx.doi.org/10.3390/molecules201018759
20. Popova T, Voycheva C, Tzankov B. Study on the influence of technological factors on drug loading of poorly water-soluble drug on MCM-41 mesoporous carrier. Pharmacia. 2020;67(4):351-356. Available from: http://dx.doi.org/10.3897/pharmacia.67. e47528
21. Baerlocher, C., McCusker, L.B. and Olson, D.H. (2007) Atlas of Zeolite Framework Types. Elsevier. Crystalline Zeolite ZSM-5 and Method of Preparing the Same. 2022.
22. Hanafi-Bojd M, Ansari L, Malaekeh-Nikouei B. Codelivery of anticancer drugs and siRNA by mesoporous silica nanoparticles. Therapeutic Delivery. 2016;7(9):649-655. Available from: http://dx.doi. org/10.4155/tde-2016-0045
23. Argauer, R.J. and Landolt, G. R. (1972) Crystalline Zeolite ZSM-5 and Method of Preparing the Same. Google Patents.
24. Thomas M, Slipper I, Walunj A, Jain A, Favretto M, Kallinteri P et al. Inclusion of poorly soluble drugs in highly ordered mesoporous silica nanoparticles. International Journal of Pharmaceutics. 2010;387(1-2):272-277. Available from: http:// dx.doi.org/10.1016/j.ijpharm.2009.12.023
25. Chen Y, Shi X, Han B, Qin H, Li Z, Lu Y et al. The Complete Control for the Nanosize of Spherical MCM-41. Journal of Nanoscience and Nanotechnology. 2012;12(9):7239-7249. Available from: http://dx.doi.org/10.1166/jnn.2012.6459
26. Hodali H, Marzouqa D. in vitro Evaluation of Zeolite Nanoparticles as Carrier for Delivery of 5-Fluorouracil. Asian Journal of Chemistry. 2016;28(7):1479-1485. Available from: http://dx.doi.org/10.14233/ajchem.2016.19724
27. Seljak K, Kocbek P, Gašperlin M. Mesoporous silica nanoparticles as delivery carriers: An overview of drug loading techniques. Journal of Drug Delivery Science and Technology. 2020;59:101906. Available from: http://dx.doi.org/10.1016/j.jddst.2020.101906
28. Sarfraz, R.M., Bashir, S., Mahmood, A., Ahsan, H., Riaz, H., Raza, H., et al. (2017) Application of Various Polymers and Polymers Based Techniques Used to Improve Solubility of Poorly Water Soluble Drugs: A Review. Acta Poloniae Pharmaceutica, 74, 347-356. Available from:
29. Murthy K, Raju V. Development and validation of new discriminative dissolution method for carvedilol tablets. Indian Journal of Pharmaceutical Sciences. 2011;73(5):527. Available from: http://dx.doi.org/10.4103/0250-474x.99000
30. Chorny M, Fishbein I, Danenberg H, Golomb G. Lipophilic drug loaded nanospheres prepared by nanoprecipitation: effect of formulation variables on size, drug recovery and release kinetics. Journal of Controlled Release. 2002;83(3):389-400. Available from: http://dx.doi.org/10.1016/S0168-3659(02)00211-0
31. Khaira R, Sharma J, Saini V. Development and Characterization of Nanoparticles for the Delivery of Gemcitabine Hydrochloride. The Scientific World Journal. 2014;2014:1-6. Available from: http://dx.doi.org/10.1155/2014/560962
32. Papadimitriou S, Bikiaris D. Novel self-assembled core–shell nanoparticles based on crystalline amorphous moieties of aliphatic copolyesters for efficient controlled drug release. Journal of Controlled Release. 2009;138(2):177-184. Available from: http://dx.doi.org/10.1016/j.jconrel.2009.05.013
33. Clayton, J. (2019) Chapter 17 - An Introduction to Powder Characterization. In: Narang, A.S. and Badawy, S.I.F., Eds., Handbook of Pharmaceutical Wet Granulation: Theory and Practice in a Quality by Design Paradigm. Academic Press, 569-613
34. Leuenberger H. The compressibility and compactibility of powder systems. International Journal of Pharmaceutics. 1982;12(1):41-55. Available from: http://dx.doi.org/10.1016/0378-5173(82)90132-6
35. Andreeva N, Radomysel'skii I, Shcherban' N. Compressibility of powders. Soviet Powder Metallurgy and Metal Ceramics. 1975;14(6):457-464. Available from: http://dx.doi.org/10.1007/BF00823503
36. Sadr M, Nabipour H. Synthesis and identification of carvedilol nanoparticles by ultrasound method. Journal of Nanostructure in Chemistry. 2013;3(1). Available from: http://dx.doi.org/10.1186/2193- 8865-3-26
37. Muhana F, Abu-Huwaij R, Khalaf N, Khalili F, Shalan N. Synthesis and Characterization of Mesoporous Silica Carrier Releasing Valsartan. Asian Journal of Chemistry. 2020;32:2927-2933. Available from: https://doi.org/10.14233/ajchem.2020.22901
38. Muhana F, AL-ani, I. AL-akayleh F. Marzouqa, D. Khalili F. A L-Khatib,H S ynthesis a nd c haracterization o f mesoporous silica and its application asdrug delivery system for glimepiride, Pharmazie. 2021;76:300-307. Available from: http://dx. Doi.org/10.1691/ ph.2021.1309.
39. Ganji R, Peyravi M, Khalili S, Jahanshahi M. Bilayer adsorptive

ceramic membranes supported cage-like mesoporous silica for hexavalent chromium removal: Experimental and DFT studies. Process Safety and Environmental Protection. 2020;143:45-54. Available from: http://dx.doi.org/10.1016/j. psep.2020.06.004

40. Zhao Q, Wang T, Wang J, Zheng L, Jiang T, Cheng G et al. Fabrication of mesoporous hydroxycarbonate apatite for oral delivery of poorly water-soluble drug carvedilol. Journal of Non-Crystalline Solids. 2012;358(2):229-235. Available from: https:// doi. org/10.1016/j.jnoncrysol.2011.09.020
41. Ben Mya O, Bita M, Louafi I, Djouadi A. Esterification process catalyzed by ZSM-5 zeolite synthesized via modified hydrothermal method. MethodsX. 2018;5:277-282. Available from: http://dx.doi.org/10.1016/j.mex.2018.03.004
42. Datt A, Burns E, Dhuna N, Larsen S. Loading and release of 5-fluorouracil from HY zeolites with varying SiO2/ Al2O3 ratios. Microporous and Mesoporous Materials. 2013;167:182-187. Available from: http://dx.doi.org/10.1016/j. micromeso.2012.09.011
43. Lin F, Lee Y, Jian C, Wong J, Shieh M, Wang C. A study of purified montmorillonite intercalated with 5-fluorouracil as drug carrier. Biomaterials. 2002;23(9):1981-1987. Available from: http://dx.doi.org/10.1016/S0142-9612(01)00325-8
44. Pardhi, D.M., Shivhare, U.D., Mathur, V.B. and Bhusari, K.P. (2010) Liquisolid Technique for Enhancement of Dissolution.
45. Cai Q, Luo Z, Pang W, Fan Y, Chen X, Cui F. Dilute Solution Routes to Various Controllable Morphologies of MCM-41 Silica with a Basic Medium. Chemistry of Materials. 2001;13(2):258-263. Available from: http://dx.doi.org/10.1021/ cm990661z
46. Datt A, El-Maazawi I, Larsen S. Aspirin Loading and Release from MCM-41 Functionalized with Aminopropyl Groups via Co-condensation or Postsynthesis Modification Methods. The Journal of Physical Chemistry C. 2012;116(34):18358-18366. Available from: http://dx.doi.org/10.1021/jp3063959
47. Geszke-Moritz M, Moritz M. APTES-modified mesoporous silicas as the carriers for poorly water-soluble drug. Modeling of diflunisal adsorption and release. Applied Surface Science. 2016;368:348-359. Available from: http://dx.doi.org/10.1016/j. apsusc.2016.02.004
48. Cheng Y, Wang L, Li J, Yang Y, Sun X. Preparation and characterization of nanosized ZSM-5 zeolites in the absence of organic template. Materials Letters. 2005;59(27):3427-3430. Available from: http://dx.doi.org/10.1016/j.matlet.2005.06.008
49. Hornauer U, Günzel R, Reuther H, Richter E, Wieser E, Möller W et al. Protection of γ-based TiAl against high temperature oxidation using ion implantation of chlorine. Surface and Coatings Technology. 2000;125(1-3):89-93. Available from: http:// dx.doi. org/10.1016/S0257-8972(99)00544-7
50. Niakan M, Asadi Z, Emami M. Binuclear Palladium Complex Immobilized on Mesoporous SBA-16: Efficient Heterogeneous Catalyst for the Carbonylative Suzuki Coupling Reaction of Aryl Iodides and Arylboronic Acids Using Cr(CO)6 as Carbonyl Source. Catalysis Letters. 2020;150(2):404-418. Available from: http:// dx.doi.org/10.1007/s10562-019-03087
51. Wu S, Hung Y, Mou C. Mesoporous silica nanoparticles as nanocarriers. Chemical Communications. 2011;47(36):9972. Available from: http://dx.doi.org/10.1039/c1cc11760b
52. Yano K, Fukushima Y. Synthesis of mono-dispersed mesoporous silica spheres with highly ordered hexagonal regularity using conventional alkyltrimethylammonium halide as a surfactantElectronic supplementary information (ESI) available: time courses of particle size and scattering intensity of samples obtained with TEOS and C16TMACl. See http://www.rsc.org/ suppdata/jm/b3/b313712k/. Journal of Materials Chemistry. 2004;14(10):1579. Available from: http://dx.doi.org/10.1039/ b313712k
53. Sápi A, Kashaboina U, Ábrahámné K, Gómez-Pérez J, Szenti I, Halasi G et al. Synergetic of Pt Nanoparticles and H-ZSM-5 Zeolites for Efficient CO2 Activation: Role of Interfacial Sites in High Activity. Frontiers in Materials. 2019;6. Available from: http:// dx.doi.org/10.3389/fmats.2019.00127
54. Trzeciak K, Chotera-Ouda A, Bak-Sypien I, Potrzebowski M. Mesoporous Silica Particles as Drug Delivery Systems—The State of the Art in Loading Methods and the Recent Progress in Analytical Techniques for Monitoring These Processes. Pharmaceutics. 2021;13(7):950. Available from: http:// x.doi. org/10.3390/pharmaceutics13070950
55. Beakawi Al-Hashemi H, Baghabra Al-Amoudi O. A review on the angle of repose of granular materials. Powder Technology. 2018;330:397-417. Available from: http://dx.doi.org/10.1016/j. powtec.2018.02.003
56. Usman S, Ejaz R, Safdar K. Formulation development and optimization of orally disintegrating tablets of montelukast sodium by Design- Expert. Tropical Journal of Pharmaceutical Research. 2018;17(9):1701. Available from: http://dx.doi. org/10.4314/tjpr.v17i9.3
57. Slotwinski J, Garboczi E. Porosity of additive manufacturing parts for process monitoring. AIP Conference Proceedings. 2014. Available from: http://dx.doi. org/10.1063/1.4864957

Supplementary Table 1: Infrared frequencies of bands of carvedilol

Carvedilol	
Vibration	*Wavenumber (cm^{-1})*
N-H stretch	3344
C-H stretching vibration (sp2)	3058
C-H stretching vibration (sp3)	2922, 2994 and 2842
C-C stretching vibration	1255–1402
C=C stretching vibration	1504–1608
C-N stretching vibration	1285–1348
In-plane C-H deformations	1000–1300
C-O stretch	1099
Ring breathing mode	784.-852.

Supplementary Table 2: Infrared frequencies of bands of MCM-41 nanoparticles and carvedilol MCM-41 loaded.

MCM-41 nanoparticles		*loaded Carvedilol on MCM-41*	
Vibration	*Wavenumber (cm^{-1})*	*Vibration*	*Wavenumber (cm^{-1})*
Hydrogen-bonded Si-O-H and water	3455	Super imposed of Si-O-H of MCM-41 with N-H stretch of Carvedilol	3410.9
Si-O-Si asymmetric stretching	1224	C-H stretching vibration (Sp2)	3066
Si-O stretching symmetric (external)	966.8	C-H stretching vibration (Sp3)	2834.8 and 2931.2
Si-O-Si symmetric stretching	806.7	C-N stretching vibration	1341.9–1394.2
H-O-H bending	1634.5	C=C stretching vibration	1506.9–1609.2
Si-OH rocking	438		

Supplementary Table 3: Infrared frequencies of bands of SBA-16 nanoparticles, coupled SBA-16 nanoparticles, carvedilol loaded on coupled SBA-16.

SBA-16 nanoparticles		*Coupled SBA-16 nanoparticles*		*loaded Carvedilol on coupled SBA-16*	
Vibration	*Wave no. (cm^{-1})*	*Vibration*	*Wave no. (cm^{-1})*	*Vibration*	*Wave no. (cm^{-1})*
Hydrogen-bonded Si-O-H and water	3450	Hydrogen-bonded Si-O-H and water	3464	Super imposed of Si-O-H of SBA-16 with N-H stretch of Carvedilol	3350
Si-O-Si asymmetric stretching (SiO4)	1070	Si-O-Si asymmetric stretching (SiO4)	1090	C-H stretching vibration (sp3)	2845 and 2930
Si-O-Si symmetric stretching (SiO4)	803	Si-O-Si symmetric stretching (SiO4)	800	Si-O-Si asymmetric stretching (SiO4) of carrier	1090
H-O-H bending	1636	H-O-H bending	1638	Si-O-Si symmetric stretching (SiO4) of carrier	800
Si-OH rocking	447	Si-OH rocking	462		
C-H Stretching vibration		N-H bending	2920		
		1560			

Supplementary Table 4: Infrared frequencies of bands of ZSM-5 nanoparticles and carvedilol-ZSM-5.

ZSM-5 nanoparticles		*ZSM-5 nanoparticles*	
Vibration	*Wavenumber (cm^{-1})*	*Vibration*	*Wavenumber (cm^{-1})*
Hydrogen-bonded Si-O-H and water	3434	Super imposed of Si-O-H of MCM-41 with N-H stretch of Carvedilol	3406
Si-O Asymmetry stretch	802	C-H stretching vibration (sp3)	2930 and 2845
Si-O-Al symmetry stretch	713	C-N stretching vibration	1310–1375
Al3+	631	C=C stretching vibration	1510–1610
Si-OH rocking	452		

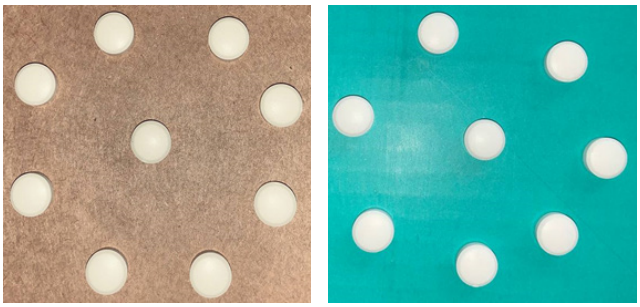

Supplementary Figure 1: The prepared tablet appearance A. F1 B. F2.